# Supporting Information

Supporting Information Corrected August 31, 2015
Hobley et al. 10.1073/pnas.1306390110

## SI Materials and Methods

**Growth Conditions.** The *Escherichia coli* and *Bacillus subtilis* strains used and constructed in this study are detailed in Table S3. Both *E. coli* and *B. subtilis* strains were routinely grown in LB medium (10 g NaCl, 5 g yeast extract, and 10 g tryptone per liter). Biofilm pellicles were grown in MSgg medium (5 mM potassium phosphate and 100 mM MOPs at pH 7.0 supplemented with 2 mM $MgCl_2$, 700 μM $CaCl_2$, 50 μM $MnCl_2$, 50 μM $FeCl_3$, 1 μM $ZnCl_2$, 2 μM thiamine, 0.5% glycerol, and 0.5% glutamate) (1) at 25 °C for 72 h; complex colonies were grown on MSgg solidified with 1.5% Select Agar (Invitrogen) at 30 °C for 48 h unless otherwise specified. Ectopic gene expression was induced with 25 μM isopropyl β-D-1-thiogalactopyranoside (IPTG). When appropriate, antibiotics were used at the following concentrations: ampicillin, 100 $\mu g \cdot mL^{-1}$; chloramphenicol, 5 $\mu g \cdot mL^{-1}$; kanamycin, 25 $\mu g \cdot mL^{-1}$; and spectinomycin, 100 $\mu g \cdot mL^{-1}$.

**Strain Construction.** All strains, plasmids, and primers used in this study are presented in Table S3. *E. coli* strain MC1061 [*F'lacIQ lacZM15 Tn10* (*tet*)] was used for the construction and maintenance of plasmids. *B. subtilis* 168 derivatives were generated by transformation of competent cells with plasmids using standard protocols (2). SPP1 phage transductions, for introduction of DNA into *B. subtilis* strain NCIB3610 (hereafter 3610), were conducted as described previously (3).

**Plasmid Construction and Site-Directed Mutagenesis.** All strains, plasmids, and primers used in this study are presented in Table S3 and were constructed using standard methods.

The plasmid for overexpression of $BslA_{42–181}$ was created as follows: $BslA_{42–181}$ was amplified from *B. subtilis* NCIB3610 genomic DNA using primers NSW1517 and NSW1537 and cloned into the vector pGEX-6P-1 using the BamHI and XhoI sites, creating the vector pNW1128. To overexpress $BslA_{48–172}$, the corresponding region of DNA was amplified from *B. subtilis* NCIB3610 genomic DNA using primers NSW1713 and NSW1714 and cloned into pGEX-6P-1 using BamHI and XhoI, creating vector pNW1196; the L98M mutation was introduced into pNW1196 using the method below, giving rise to vector pNW1160, which was used for crystallography (see below).

Single amino acid substitutions were created in the vectors using PCR site-directed mutagenesis with the appropriate primer pairs from Table S3, using PCR amplification conditions calculated according to the Stratagene Quikchange manual using KOD Hot Start DNA Polymerase (Novagen). The PCR products were then treated with DpnI and transformed into competent *E. coli* MC1061 cells (Table S3).

To prepare vectors for expression of site-directed mutant forms of BslA in *B. subtilis*, the *bslA* gene was removed from the vector pNW518 using HindIII and SphI and cloned into the high-copy-number vector pUC19, creating the vector pNW690. This vector was then used for the site-directed mutagenesis PCRs, before the *bslA* coding region was excised using HindIII and SphI and cloned into pDR111 in preparation for transformation into *B. subtilis* 168 and recombination into the *amyE* locus.

**Immunofluorescence.** For the purpose of fluorescence microscopy, strains that expressed the gene encoding the green fluorescent protein from an IPTG-inducible promoter were used (Table S3). Biofilm pellicles were grown in six-well microtiter dishes (Greiner) containing 10 mL of MSgg growth medium (described above) at 37 °C for 16 h. Coverslips (18 × 18 mm, 1.5 thickness) were coated with concanavalin A (Sigma) and placed under the pellicle. The spent growth media was removed to allow the pellicle to settle on the coverslip. A 5-min incubation allowed binding of the cells to the concanavalin A. The pellicle was fixed with 150 μL of 4% paraformaldehyde in PBS for 10 min. The coverslips were washed three times with PBS and blocked for several hours in 2% fish skin gelatin (Sigma) in PBS. After three sequential washes with PBS, 150 μL of rabbit anti-BslA antibodies (4) diluted 1/10 in AbDil [1× Tris-buffered saline (TBS), 2% BSA, and 0.1% azide] (5) was applied and coverslips were incubated overnight at 4 °C. Next, the coverslips were washed three times with PBS and incubated for 90 min in 150 μL of DyLight594-conjugated Affinity Pure Donkey Anti-Rabbit IgG (H+L) secondary antibody (Jackson ImmunoResearch) diluted 1/150 in AbDil. The coverslips were washed three times with PBS and mounted on a microscope slide on the anti-fade containing mounting medium [0.5% p-Phenylenediamine (Free base; Sigma), 20 mM Tris (pH 8.8), and 90% glycerol] (5) and sealed with nail varnish.

Complex colonies were grown on MSgg solidified with 1.5% agar as described above. A quarter section of the colony (after 48 h of growth) was excised with a number 10 surgical scalpel and placed into optimum cutting temperature compound (Agar Scientific) and frozen in iso-pentene chilled with liquid nitrogen. Cross-sections (10 μm) of the colony were cut using a Leica CM3050 S cryomicrotome. The sections were transferred onto SuperFrost Ultra Plus adhesion microscope slides (VWR). The immunofluorescence staining was performed as detailed above. A drop of the mounting medium was applied onto a labeled section of the colony and the slide was placed under a 1.5-thickness cover glass (22 × 22 mm) and sealed with nail varnish. The slides were stored at −20 °C before analysis. Samples were imaged using a Zeiss LSM700 confocal scanning laser microscope fitted with 488-nm and 555-nm lasers and an EC Plan-Neofluar 40×/ 1.30 oil differential interference contrast (DIC) M27 or an alpha Plan-Apochromat 100×/ 1.49 oil DIC objective. The optical section thickness was 200 nm. During each experiment the laser settings, scanning speed, photomultiplier tube gains, and pinhole settings were kept constant for all acquired image stacks. Images were captured using Zen2009 software and 2D image analysis was conducted using the OMERO platform (www.openmicroscopy.org) (6). All figures were assembled in Canvas 12 (ACD Systems).

**Quantification of the Abundance of Fluorescence.** To assess the abundance of fluorescence throughout the depth of the pellicle, the images acquired by confocal microscopy were stored and annotated with regions of interest in OMERO (6). Following this, automated batch image analysis was performed with bespoke software written in Matlab (MathWorks) via the OMERO API (code available upon request). Briefly, for each field of view, the Z-stack of GFP (representing the cells) and DyLight594 (representing the immunolabeled BslA) channels was downloaded into Matlab. The signal in each channel was segmented from background using the Otsu method (7). For every Z-section, for each fluorescence channel, the number of segmented pixels and the total number of pixels was stored in a vector (note: the total number of pixels possible in each Z-section is 512 × 512). The first Z-section containing a signal from GFP was regarded as Z = 0 and the vectors were aligned in a matrix to generate a common reference point. The matrix of pixel counts was converted to a spreadsheet. The graph presented here (Fig. S1*A*)

was produced in SigmaPlot 12.0 where total average pixel count (a measurement of the abundance of signal) was plotted against the depth of the biofilm in micrometers. The average was calculated from 36 independent images.

**Single-Cell Quantification of *bslA* Expression.** Complex colonies were grown on MSgg agar plates for 18 h at 37 °C and harvested as previously described (8, 9). In brief, the cells were collected and suspended in 500 μL PBS and disrupted by passing through a 23× 1 needle three times. The cells were then fixed by addition of 4% paraformaldehyde for 7 min, then the cells were then collected by centrifugation at 17,000 × *g* for 1 min and suspended in 500 μL sterile PBS and the matrix disrupted by gentle sonication. For flow cytometry analysis 1 μL of this cell suspension was added to 1 mL PBS with 1% (wt/vol) BSA (VWR) and cells were measured on a BD FACS Calibur (BD Biosciences) with GFP fluorescence measured using 488-nm excitation and detection at 530 ± 30 nm. The data were collected using Cell Quest Pro (BD Biosciences) and further analyzed using FlowJo version 4.3. For microscopy analysis, 2 μL of the cell suspension was spotted onto a 1.5% agarose pad and imaged using a DeltaVision Core widefield system (Applied Precision) consisting of an Olympus IX71 inverted microscope with an Olympus 100× 1.35 N.A. lens and CoolSNAPHQ camera (Photometrics). Images were acquired with DIC and GFP fluorescence optics including a 100-W mercury lamp and a FITC filter set (excitation, 490/20; emission, 528/38) with an exposure time of 400 ms. DIC images were acquired with a light-emitting diode transmitted light source (Applied Precision) at 32% intensity. Images were rendered and analyzed using OMERO software (http://openmicroscopy.org) (6). All figures were assembled in Canvas 12 (ACD Systems).

**Protein Purification.** For overexpression of BslA variants fused to GST, which were separated with a tobacco etch virus (TEV) protease site, the appropriate pGEX-6P-1 derived plasmids (Table S3) were transformed into *E. coli* BL21 (DE3) pLysS. The transformed cells were pregrown in LB broth overnight and inoculated into autoinduction media (10) supplemented with ampicillin (100 μg/mL) at a ratio of 1:1,000 (vol:vol). The cultures were incubated at 30 °C with agitation until $OD_{600} \approx 0.9$ when the temperature was reduced to 18 °C and incubated overnight. The cells were collected by centrifugation (4,000 × *g* for 45 min) and resuspended in the purification buffer [50 mM Hepes (pH 7.5) and 250 mM NaCl] supplemented with Complete EDTA-Free Proteinase Inhibitors mixture (Roche) at the ratio of 20 mL of buffer per 7 mL of the pelleted cells. The cells were lysed using an Emulsiflex cell disruptor by applying 15,000 psi of pressure twice to each sample. Cell debris and unlysed cells were removed by centrifugation (27,000 × *g* for 20 min). The cleared lysate was mixed with 1.5 mL (per 1 L of culture) Glutathione Sepharose 4B (GE Healthcare) and gently agitated at 4 °C for 4 h to allow GST binding to the beads. The lysate was loaded onto a single-use, 25-mL gravity flow column (Bio-Rad) and allowed to flow through. The collected beads were washed twice with 25 mL of the purification buffer then transferred to 50-mL falcon tubes and incubated overnight at 4 °C with agitation in 25 mL of the purification buffer supplemented with 1 mM DTT and 0.5 mg of purified TEV protease to release BslA from the GST tag. The solution containing released BslA, TEV protease, unbound GST, and the beads was loaded onto the gravity flow columns and the flow-through collected. The beads were regenerated by agitation for 2 h in 25 mL of the purification buffer supplemented with 50 mM reduced glutathione (Sigma), washed three times with 50 mL of the purification buffer by centrifugation (1,000 × *g* for 3 min). The protein suspension was added to the regenerated beads together with 250 μL of Ni-nitrilotriacetic acid agarose (Qiagen) slurry to remove the TEV protease. The mixture was incubated with gentle agitation overnight at 4 °C then passed through a gravity flow column, and the purified BslA was collected in the flow-through and analyzed by SDS/PAGE. The purified protein was concentrated using VivaSpin concentrators (Sartorius) and the buffer exchanged with 25 mM phosphate buffer (pH 7).

**Pendant Drop Experiments and Surface Wrinkle Relaxation Quantification.** The interfacial tension of protein samples (0.2 mg/mL, pH 7, in 25 mM phosphate buffer) against the oil glyceryl trioctanoate was measured using the pendant drop method (11, 12) with a KrüssEasyDrop tensiometer (Krüss). The needle diameter was 1.8 mm and the droplet volume was 40 μL. A droplet of the protein in aqueous solution was expelled into the oil and allowed to equilibrate at room temperature for 20 min. Images were acquired at 0.4-s (L77K and L79K) or 1 s (wild type and L76K) intervals using a digital camera. Wrinkle relaxation experiments were performed following compression of the droplet, which was achieved by retracting 5 μL of the aqueous solution. In cases in which a film formed at the oil/water interface, compression causes visible wrinkles to form on the surface of the droplet. As shown in Fig. 4 and Fig. S2 and Movies S1–S4, wrinkles manifest as light and dark regions on the droplet surface; in the absence of an elastic film the surface is uniformly one color. After formation, the wrinkles were monitored over a period of 10 min to investigate film relaxation. The videos of the recordings were split into individual frames and image analysis was performed on each frame. We selected a line profile across the neck of the droplet, where wrinkles are most apparent, and plotted the grayscale values (from 0 to 255) of each pixel along this line using the ImageJ software package (http://rsbweb.nih.gov/ij/). After each frame in a sequence had been analyzed with a line profile, a single high-contrast wrinkle on each droplet was selected and followed over time. To plot the relaxation rate, the grayscale value of the pixels was normalized to values between 0 and 100 and background corrected. The value 0 represents the fully relaxed, unwrinkled state, and the value 100 represents a wrinkle.

**CD Spectropolarimetry.** A Jasco J-810 CD spectropolarimeter was used to perform CD experiments. Protein samples (0.2 mg/mL, pH 7, 25 mM phosphate buffer) were analyzed in a 1-cm path length quartz cuvette. Each spectrum is the average of five scans, acquired at a scan rate of 20 nm/min using a digital integration time of 1 s.

**Protein Expression and Purification for Crystallization.** The plasmid pNW1160 pGEX-6P-1-$bslA_{48–172,\ L98M}$ (Table S4) was transformed into *E. coli* B834-DE3 cells. Cultures (100 mL) were grown overnight in LB containing ampicillin (100 μg/mL). The cells were pelleted, washed three times in 100 mL of M9 (minimum) media, and resuspended in 10 mL of M9 media plus L-selenomethionine (Molecular Dimensions). This was then used to inoculate 1 L of M9 media plus L-selenomethionine containing ampicillin. The cells were grown at 37 °C to $OD_{600}$ of 0.6 and expression was initiated by the addition of 100 μM isopropyl-D-thiogalactopyranoside (IPTG). The cells were cultured for an additional 18 h at 18 °C, harvested by centrifugation at 2,250 × *g* for 30 min, and the cell pellet from each liter of culture was suspended in 40 mL of M9 media and subjected to another round of centrifugation. The resulting cell pellets were flash-frozen in liquid nitrogen, thawed at 37 °C in a water bath, and suspended in 10 mL of lysis buffer [50 mM Hepes/250 mM NaCl (pH 7.5) and 0.5 tablet of complete protease inhibitor mixture tablets (Roche)]. Cells were lysed by the addition of 5 mg of DNase-1, incubated for 15 min on ice, and passed three times through an EmulsiFlex-C3 homogenizer (Avestin, Inc.). The

lysate was centrifuged at 40,000 × *g* for 30 min and filtered through a 0.45-μm filter. The supernatant was incubated for 2 h at 4 °C on a rotating platform with Glutathione-Sepharose (GE Healthcare) beads prewashed with lysis buffer in a ratio of 1 mL of beads per liter of bacterial culture. The beads were then incubated with PreScission protease (200 mg of protease per milliliter of beads) at 4 °C for 18 h in protease inhibitor-free lysis buffer. The supernatant of the beads and a subsequent wash were passed over a Bio-Rad 20-mL disposable column to remove the beads. The eluted protein was concentrated to 4 mL using a VivaScience 5000 molecular weight cut-off concentrator. The protein concentration and purity was determined by Bradford assay and SDS/PAGE. The protein was methylated following the protocol previously described (11). The methylated protein was concentrated to 2 mL and loaded onto a Superdex 75, 26/60 gel filtration column. The resulting fractions were verified by SDS/PAGE and pooled. This was concentrated to 25 mg/mL, as verified by a Bradford assay and absorbance at 280 nm. The sitting-drop vapor diffusion method was used to produce crystals by mixing 1 μL of protein solution with 1 μL of a mother liquor solution (1.9 M $Li_2SO_4$ and 0.1 M Hepes, pH 7.5). Crystal growth improved with the addition of 10 μL of 100 mM glucose to 100 μL of mother liquor. Rod-shaped crystals grew within 5 d. Crystals were frozen in a nitrogen gas stream cooled to 100 K after being cryoprotected transiently in mother liquor containing 15% glycerol.

**Data Collection, Structure Solution, and Refinement.** Data were collected on the $BslA_{48–172\text{-}L98M}$ selenomethionine derivative as shown in Table S1. A single-wavelength anomalous dispersion experiment was carried out at beamline I-02 at the Diamond Light Source. Data were processed using XDS (12) and SCALA (13). Phasing was performed using PHENIX AutoSol (14), which identified 20 selenium sites with a figure of merit of 0.45. Solvent flattening was then performed with PHENIX resolve using a solvent content of 63%, assuming 10 molecules per asymmetric unit. This yielded a readily interpretable electron density map, from which PHENIX AutoBuild (15) was able to automatically build. Further refinement [with REFMAC (16) and PHENIX Refine (17)] and model building with Coot (18) then yielded the final model with the statistics shown in Table S1. Figures were made with PYMOL (19).

**Western Blot Analysis.** Entire complex colonies were gathered from the agar plate using a sterile loop and suspended in 500 μL of BugBuster Master Mix (Novagen) and disrupted by passing through a 23 × 1 needle three times followed by gentle sonication (8, 9). The samples were then incubated at room temperature with agitation for 20 min, and the insoluble cell debris was removed by centrifugation at 17,000 × *g* for 10 min at 4 °C. The total protein concentration was measured using Bio-Rad DC Protein Assay and 1.25 μg of total protein was loaded per well on a 14% SDS/PAGE gel before transfer onto PVDF membrane (Millipore) by electroblotting. Pellicles were grown in 10 mL of culture as described previously (1). The pellicle was separated into two fractions: pellicle and media. The entire pellicle and media was centrifuged at 5,000 × *g* for 10 min and the pellet and supernatant separated. The pellet was then termed the pellicle fraction (containing both cells and matrix) and was prepared in the same way as the complex colonies described above. The supernatant was the designated the media fraction and filtered through a 0.45-μm syringe filter (Sartorius); 5 mL of this was then added to 5 mL of a 50% chloroform: 50% (vol/vol) methanol solution and centrifuged for 5 min at 5,000 × *g*. The proteins from the phase interface were collected and washed with 100% methanol and air dried. The precipitants were dissolved in 500 μL SDS/PAGE loading dye and 5 μL loaded onto a 14% SDS/PAGE gel and transferred onto PVDF membrane (Millipore) by electroblotting. The membranes were incubated for 1 h in 3% (wt/vol) powdered milk in TBS [20 mM Tris·HCl (pH 8.0) and 0.15 M NaCl]. This was followed by an overnight incubation with the primary antibody raised against TasA at a dilution of 1:25,000 or affinity-purified antibody (4) raised against BslA at a dilution of 1:500 in 3% powdered milk wash buffer (TBS + 0.05% Tween 20). The membrane was washed using wash buffer and incubated for 45 min with the secondary antibody conjugated to horseradish peroxidize [goat anti-rabbit (Pierce)] at a dilution of 1:5,000. The membrane was washed, developed, and exposed to X-ray film.

**Colony Hydrophobicity Contact Angle Measurements.** Complex colonies were grown on MSgg agar plates (as described above) for 48 h at 30 °C. A 5-μL drop of sterile double-distilled water was placed on the colony using the KrüssEasyDrop tensiometer (Krüss). The drop was allowed to equilibrate for 5 min before the contact angles were imaged and measured.


1. Branda SS, González-Pastor JE, Ben-Yehuda S, Losick R, Kolter R (2001) Fruiting body formation by *Bacillus subtilis*. *Proc Natl Acad Sci USA* 98(20): 11621–11626.
2. Harwood CR, Cutting SM (1990) *Molecular Biological Methods for Bacillus* (Wiley, Chichester, UK).
3. Verhamme DT, Kiley TB, Stanley-Wall NR (2007) DegU co-ordinates multicellular behaviour exhibited by *Bacillus subtilis*. *Mol Microbiol* 65(2):554–568.
4. Ostrowski A, Mehert A, Prescott A, Kiley TB, Stanley-Wall NR (2011) YuaB functions synergistically with the exopolysaccharide and TasA amyloid fibers to allow biofilm formation by *Bacillus subtilis*. *J Bacteriol* 193(18):4821–4831.
5. Cramer L, Desai A (1995) Fluorescence procedures for the actin and tubulin cytoskeleton in fixed cells. Available at http://mitchison.med.harvard.edu/protocols/general/Fluorescence%20Procedures%20for%20the%20Actin%20and%20Tubulin%20Cytoskeleton%20in%20Fixed%20Cells.pdf. Accessed July 18, 2013.
6. Allan C, et al. (2012) OMERO: Flexible, model-driven data management for experimental biology. *Nat Methods* 9(3):245–253.
7. Otsu N (1979) Threshold selection method from gray-level histograms. *Ieee T Syst Man Cyb* 9(1):62–66.
8. Murray EJ, Strauch MA, Stanley-Wall NR (2009) SigmaX is involved in controlling Bacillus subtilis biofilm architecture through the AbrB homologue Abh. *J Bacteriol* 191 (22):6822–6832.
9. Vlamakis H, Aguilar C, Losick R, Kolter R (2008) Control of cell fate by the formation of an architecturally complex bacterial community. *Genes Dev* 22(7):945–953.
10. Studier FW (2005) Protein production by auto-induction in high density shaking cultures. *Protein Expr Purif* 41(1):207–234.
11. Walter TS, et al. (2006) Lysine methylation as a routine rescue strategy for protein crystallization. *Structure* 14(11):1617–1622.
12. Kabsch W (2010) Xds. *Acta Crystallogr D Biol Crystallogr* 66(Pt 2):125–132.
13. Winn MD, et al. (2011) Overview of the CCP4 suite and current developments. *Acta Crystallogr D Biol Crystallogr* 67(Pt 4):235–242.
14. Terwilliger TC, et al. (2009) Decision-making in structure solution using Bayesian estimates of map quality: The PHENIX AutoSol wizard. *Acta Crystallogr D Biol Crystallogr* 65(Pt 6):582–601.
15. Terwilliger TC, et al. (2008) Iterative model building, structure refinement and density modification with the PHENIX AutoBuild wizard. *Acta Crystallogr D Biol Crystallogr* 64(Pt 1):61–69.
16. Murshudov GN, Vagin AA, Dodson EJ (1997) Refinement of macromolecular structures by the maximum-likelihood method. *Acta Crystallogr D Biol Crystallogr* 53(Pt 3):240–255.
17. Adams PD, et al. (2010) PHENIX: A comprehensive Python-based system for macromolecular structure solution. *Acta Crystallogr D Biol Crystallogr* 66(Pt 2):213–221.
18. Emsley P, Cowtan K (2004) Coot: Model-building tools for molecular graphics. *Acta Crystallogr D Biol Crystallogr* 60(Pt 12 Pt 1):2126–2132.
19. DeLano WL (2004) Use of PYMOL as a communications tool for molecular science. *Abstr Pap Am Chem S* 228:U313–U314.

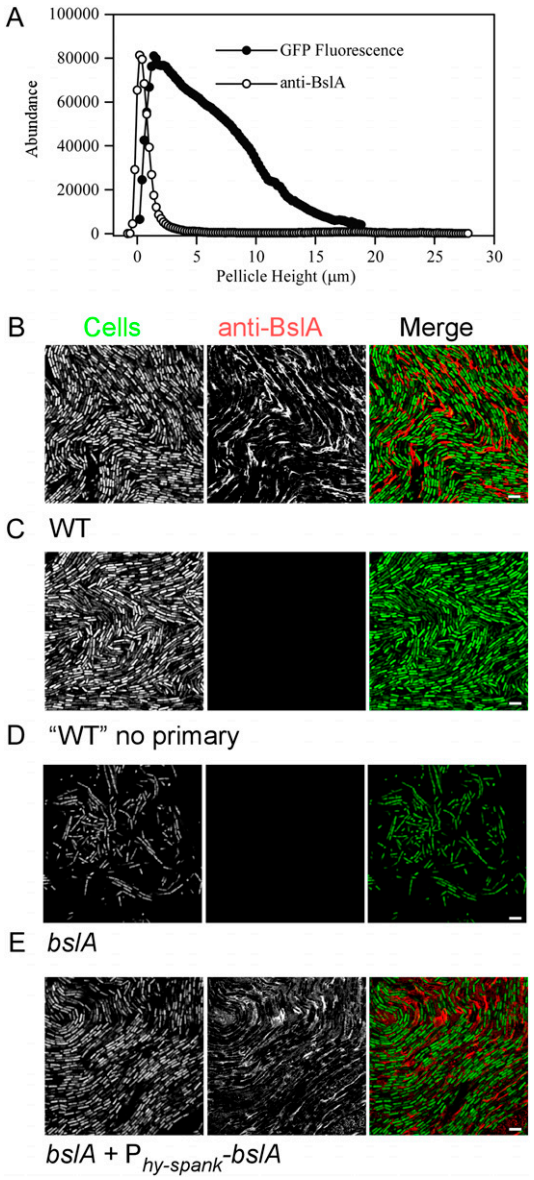


**Fig. S1.** Immuno-labeling controls for in vivo pellicle biofilm analysis. (*A*) Average values of abundance of the fluorescent signal for GFP, depicting cells in the biofilm as solid circles, and DyLight594, representing immuno-labeled BslA as open circles, in each of the Z-sections acquired from the wild-type cells (3610, *sacA*::$P_{hy\text{-}spank}$-*gfp*; NRS1473). The signal abundance was calculated from pixel population for each of the *xy* images and plotted against the height (z-number) of the pellicle, where 0 μm depicts the first *xy* section containing GFP signal at the base of the pellicle biofilm. Typical 0.2-μm *xy* sections of (*B*) a wild-type pellicle (NRS1473; 3610, *sacA*::$P_{hy\text{-}spank}$-*gfp*) such as that shown in Fig. 2, (*C*) a wild-type pellicle processed in an identical manner, except without the primary anti-BslA antibody, (*D*) the *bslA* mutant strain (NRS3812; 3610, *bslA*::*cat*, *sacA*::$P_{hy\text{-}spank}$-*gfp*), and (*E*) the complemented *bslA* strain (NRS3790; 3610, *bslA*::*cat*, *amyE*::$P_{hy\text{-}spank}$-*bslA*, *sacA*::$P_{hy\text{-}spank}$-*gfp*). Fluorescence from the GFP within the cells is presented in white in the left column or false-colored green in the merged image. Fluorescence associated with DyLight594, representing immuno-labeled BslA staining, is presented in white in the middle column or false-colored red in the merged image. (Scale bars, 5 μm.)

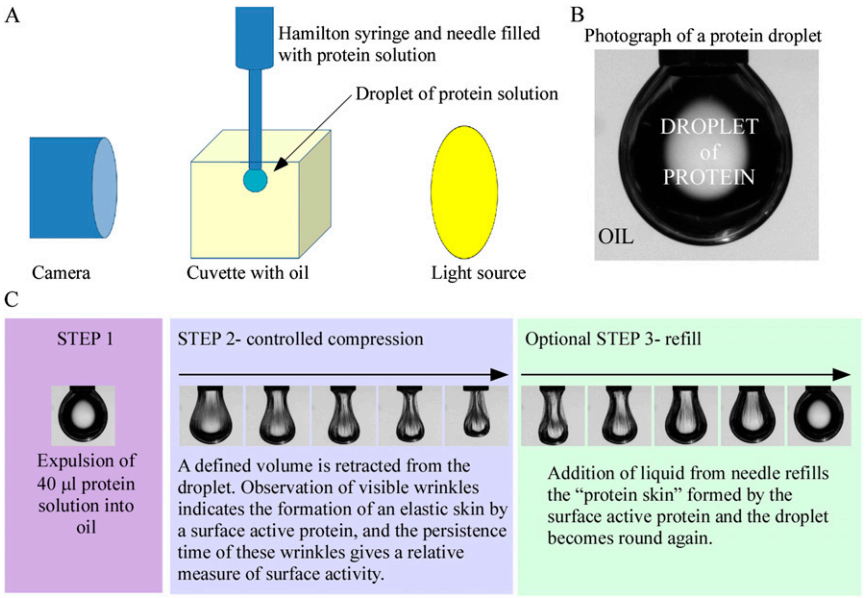


**Fig. S2.** Pendant drop analysis of surface active proteins. (*A*) Experimental setup for collection of data. (*B*) Example of a 40-µL BslA protein droplet expelled into oil. (*C*) Detailed explanation of the methodology used to examine the surface activity of BslA.

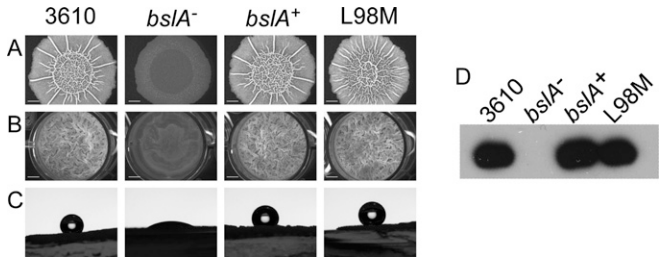


**Fig. S3.** Analysis of the in vivo effects of introduction of the L98M substitution into BslA. Biofilm formation of the wild-type (NCIB3610), *bslA* mutant (NRS2097; 3610, *bslA*::cat), complemented *bslA* mutant (NRS2299; 3610, *bslA*::cat, *amyE*::$P_{hy\text{-}spank}$-*bslA*), and L98M mutant (NRS4520; 3610, *bslA*::*cat*, *amyE*::$P_{hy\text{-}spank}$-$bslA_{L98M}$) strains. (*A*) Complex colony morphology and (*B*) pellicle morphology of each strain. (*C*) Five-microliter droplets of water were placed on the surface of the complex colonies and allowed to equilibrate for 5 min before photography; the *bslA* mutant colony is shown to be subjected to wetting by the water droplet. (*D*) Western blot analysis of total protein isolated from complex colonies using a BslA-specific antibody showing the presence of wild-type levels of BslA protein in the L98M mutant colony.

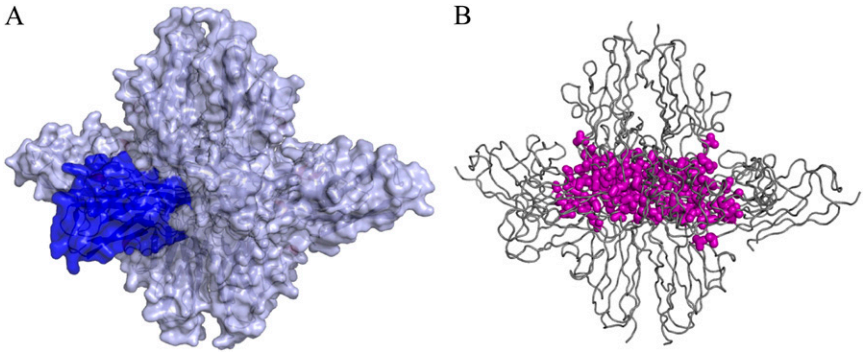


**Fig. S4.** Asymmetric unit crystal packing of BslA. Ten monomers of BslA form a crystal in space group $P2_12_12_1$. (*A*) The surface of the decamer, with a single BslA monomer highlighted in blue. (*B*) C-α representation of the decamer of BslA, with each of the leucines, isoleucines, and valines contained within the hydrophobic cap shown in magenta.

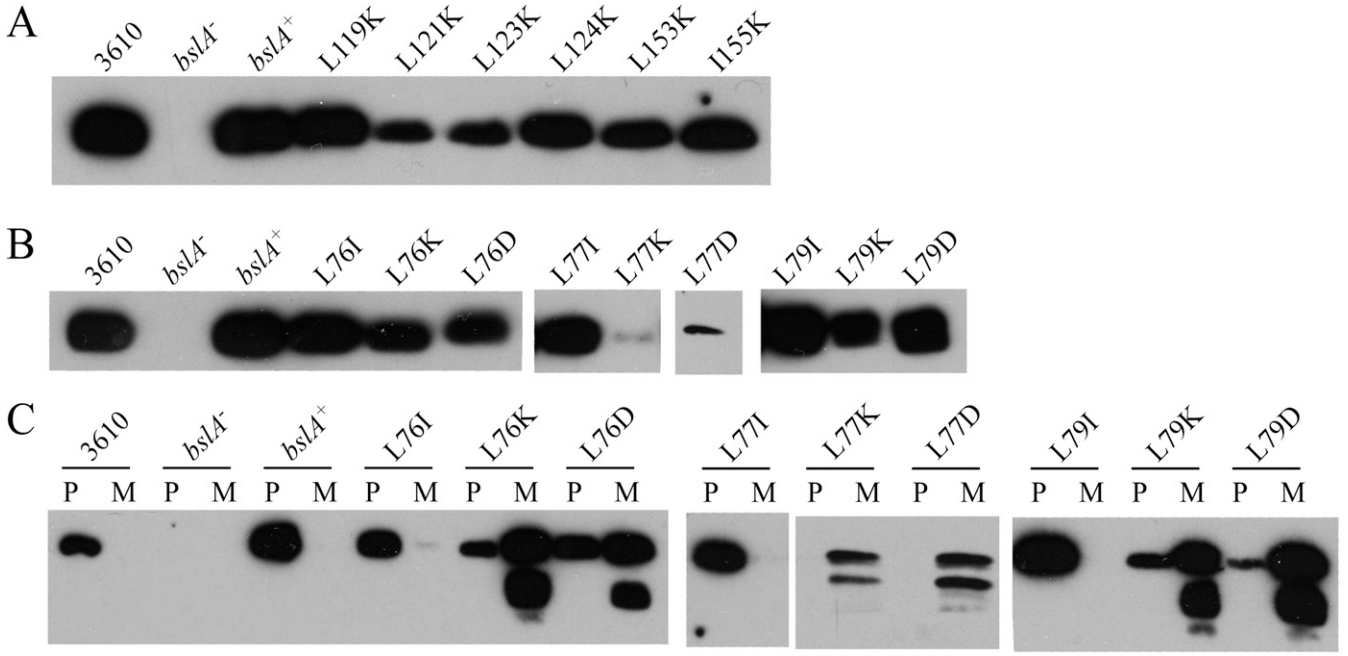


**Fig. S5.** Protein production and stability of in vivo BslA hydrophobic cap mutants. Western blot analysis using a BslA-specific primary antibody of protein extracted from whole complex colonies of (*A*) CAP2 and CAP3 mutants (as shown in Fig. 6*A*) and (*B*) CAP1 mutants (Fig. 6*D*). Colonies were grown for 48 h at 30 °C before extraction. (*C*) Pellicles of CAP1 mutant strains, grown for 18 h at 37 °C, were separated into pellicle (P, containing both cells and the biofilm matrix) and media (M) fractions. Western blots were probed with a BslA-specific primary antibody. Pellicles with wild-type morphology show that most BslA protein is found within the P fraction, whereas those with altered pellicle morphology have BslA protein in both the P and M fractions. When BslA is present in the media a second, lower-molecular-weight degradation product appears.

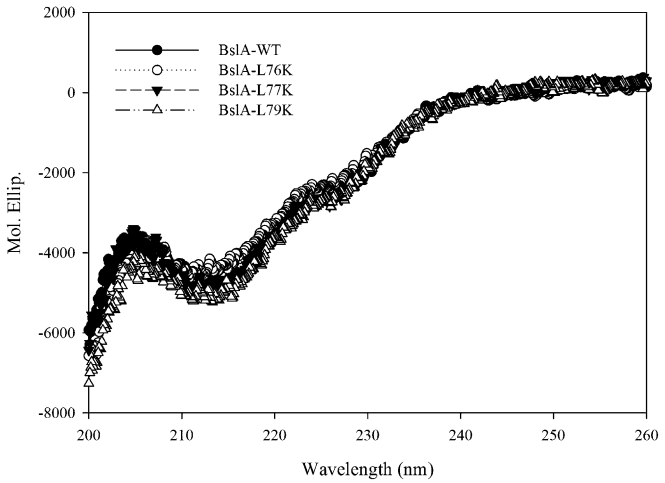


**Fig. S6.** CD analysis of BslA. Purified $BslA_{42–181}$ protein was analyzed by CD spectropolarimetry and compared with $BslA_{42–181}$ protein containing the CAP1 mutations L76K, L77K, and L79K, showing no significant changes in protein topology caused by the leucine-to-lysine substitutions.

**Table S1. Crystallography data collection and refinement statistics**

| $BslA_{48–172}$-L98M-SeMet single anomalous dispersion | |
|---|---|
| Wavelength, Å | 0.9797 |
| Resolution, Å | 77.19–1.91 (1.978–1.91) |
| Space group | $P\ 2_1\ 2_1\ 2_1$ |
| Unit cell | |
| *a*, Å | 69.70 |
| *b*, Å | 95.98 |
| *c* , Å | 259.81 |
| No. of reflections | 1,834,313 (137,083) |
| No. of unique reflections | 135,912 (13,446) |
| $I/\sigma$ ($I$) | 18.04 (4.27) |
| Completeness, % | 100.0 (100.0) |
| Redundancy | 13.3 (13.5) |
| Wilson B-factor | 24.7 |
| $R_{merge}$, % | 0.094 (0.669) |
| Rmsd from ideal geometry | |
| Bond distance, Å | 0.011 |
| Bond angle, ° | 1.37 |
| $R_{work}$, % | 16.5 |
| $R_{free}$, % | 19.9 |
| No. of residues | 2693 |
| No. of water molecules | 1,411 |
| B factors, $Å^2$ | |
| Overall | 28.7 |
| Protein | 27.5 |
| Ligand | 37.1 |
| Ramachandran analysis | |
| Favored, % | 99.8 |
| Outliers, % | 0 |

**Table S2. In vivo characterization of the hydrophobic cap**

| Mutation | Colony morphology | Pellicle morphology | Water drop assay (mean contact angle ± SE) |
|---|---|---|---|
| Wild-type | Wild-type | Wild-type | Nonwetting 128.9° ± 1.3 |
| *bslA* | Null | Null | Wetting 24.7° ± 2.7 |
| *bslA*$^+$ | Wild-type | Wild-type | Nonwetting 127.2° ± 3.4 |
| L76 | | | |
| I | Wild-type | Wild-type | Nonwetting 124.8° ± 2.2 |
| K | Intermediate (almost null) | Null | Nonwetting 120.2° ± 13.1 |
| D | Intermediate | Intermediate | Nonwetting 127.6° ± 10.7 |
| L77 | | | |
| I | Wild-type | Wild-type | Nonwetting 118.0° ± 8.3 |
| K | Null | Null | Wetting 49.6° ± 4.5 |
| D | Null | Null | Wetting 40° ± 0.4 |
| L79 | | | |
| I | Wild-type | Wild-type | Nonwetting 122.1° ± 7.4 |
| K | Null | Null | Wetting 23.7° ± 5.0 |
| D | Null | Null | Wetting 18.5° ± 7.4 |
| L119K | Wild-type | Wild-type | Nonwetting 115.1° ± 8.0 |
| L121K | Intermediate | Null | Nonwetting 128.5° ± 1.0 |
| L123K | Intermediate (almost null) | Null | Nonwetting 130.5° ± 2.0 |
| L124K | Intermediate | Wild-type | Nonwetting 133.4° ± 0.8 |
| L153K | Intermediate | Null | Nonwetting 123.9° ± 1.7 |
| I155K | Intermediate | Null | Nonwetting 128.9° ± 1.9 |

**Table S3. Full list of strains, plasmids, and primers used in this study**

| Strain, plasmid, or primer | Relevant genotype/description | Source/construction*,† |
|---|---|---|
| Strain | | |
| MC1061 | *E. coli F'lacIQ lacZM15 Tn10* (*tet*) | *E. coli* Genetic Stock Centre |
| BL21 (DE3) | F– *ompT hsdS*$_B$($r_B^-$, $m_B^-$) *gal dcm* (DE3) | 1 |
| B834 (DE3) | $F^-$ *ompT hsdS*$_B$($r_B^-$ $m_B^-$) *gal dcm met* (DE3) | Novagen |
| NCIB3610 | prototroph | BGSC |
| 168 | *trpC2* | BGSC |
| JH642 | *trpC2 pheA1* | 2 |
| NRS1471 | JH642 *sacA*::P$_{hy\text{-}spank}$-*gfpmut2 (kan)* | 3 |
| NRS1473 | 3610 *sacA*::P$_{hy\text{-}spank}$-*gfpmut2 (kan)* | SPP1 NRS1471 → 3610 |
| NRS2097 | 3610 *bslA*::*cat* | 4 |
| NRS2289 | 3610 *sacA*::P$_{bslA}$-*gfpmut2 (kan)* | 5 |
| NRS2299 | 3610 *bslA*::*cat amyE*::P$_{hy\text{-}spank}$-*bslA-lacI (spc)* | 4 |
| NRS2394 | 3610 *sacA*::P$_{tapA}$-*gfpmut2 (kan)* | 6 |
| NRS3790 | 3610 *bslA*::*cat amyE*::P$_{hy\text{-}spank}$-*bslA-lacI* (spc) *sacA*::P$_{hy\text{-}spank}$-*gfpmut2 (kan)* | SPP1 NRS1471 → NRS2299 |
| NRS3812 | 3610 *bslA*::*cat sacA*::P$_{hy\text{-}spank}$-*gfpmut2 (kan)* | SPP1 NRS1471 → NRS2097 |
| NRS3820 | 3610 *bslA*::*cat amyE*::P$_{hy\text{-}spank}$-*bslA*$_{L76I}$-*lacI (spc)* | SPP1 NRS3969 → NRS2097 |
| NRS3969 | 168 *amyE*::P$_{hy\text{-}spank}$-*bslA*$_{L76I}$-*lacI (spc)* | pNW1104 →168 |
| NRS4156 | 168 *amyE*::P$_{hy\text{-}spank}$-*bslA*$_{L76D}$-*lacI (spc)* | pNW1143 →168 |
| NRS4158 | 168 *amyE*::P$_{hy\text{-}spank}$-*bslA*$_{L76K}$-*lacI (spc)* | pNW1144 →168 |
| NRS4171 | 3610 *bslA*::*cat amyE*::P$_{hy\text{-}spank}$-*bslA*$_{L76D}$-*lacI (spc)* | SPP1 NRS4156 → NRS2097 |
| NRS4175 | 3610 *bslA*::*cat amyE*::P$_{hy\text{-}spank}$-*bslA*$_{L76K}$-*lacI (spc)* | SPP1 NRS4158 → NRS2097 |
| NRS4437 | 168 *amyE*::P$_{hy\text{-}spank}$-*bslA*$_{L79I}$-*lacI (spc)* | pNW1158 →168 |
| NRS4439 | 168 *amyE*::P$_{hy\text{-}spank}$-*bslA*$_{L79D}$-*lacI (spc)* | pNW1157 →168 |
| NRS4442 | 3610 *bslA*::*cat amyE*::P$_{hy\text{-}spank}$-*bslA*$_{L79I}$-*lacI (spc)* | SPP1 NRS4437 → NRS2097 |
| NRS4446 | 3610 *bslA*::*cat amyE*::P$_{hy\text{-}spank}$-*bslA*$_{L79D}$-*lacI (spc)* | SPP1 NRS4439 → NRS2097 |
| NRS4475 | 168 *amyE*::P$_{hy\text{-}spank}$-*bslA*$_{L79K}$-*lacI (spc)* | pNW1165 →168 |
| NRS4481 | 3610 *bslA*::*cat amyE*::P$_{hy\text{-}spank}$-*bslA*$_{L79K}$-*lacI (spc)* | SPP1 NRS4475 → NRS2097 |
| NRS4515 | 168 *amyE*::P$_{hy\text{-}spank}$-*bslA*$_{L98M}$-*lacI (spc)* | pNW1178 →168 |
| NRS4516 | 168 *amyE*::P$_{hy\text{-}spank}$-*bslA*$_{L77I}$-*lacI (spc)* | pNW1179 →168 |
| NRS4517 | 168 *amyE*::P$_{hy\text{-}spank}$-*bslA*$_{L77K}$-*lacI (spc)* | pNW1180 →168 |
| NRS5065 | 168 *amyE*::P$_{hy\text{-}spank}$-*bslA*$_{L77D}$-*lacI (spc)* | pNW1461 →168 |
| NRS4520 | 3610 *bslA*::*cat amyE*::P$_{hy\text{-}spank}$-*bslA*$_{L98M}$-*lacI (spc)* | SPP1 NRS4515 → NRS2097 |
| NRS4522 | 3610 *bslA*::*cat amyE*::P$_{hy\text{-}spank}$-*bslA*$_{L77I}$-*lacI (spc)* | SPP1 NRS4516 → NRS2097 |
| NRS4524 | 3610 *bslA*::*cat amyE*::P$_{hy\text{-}spank}$-*bslA*$_{L77K}$-*lacI (spc)* | SPP1 NRS4517 → NRS2097 |
| NRS5071 | 3610 *bslA*::*cat amyE*::P$_{hy\text{-}spank}$-*bslA*$_{L77D}$-*lacI (spc)* | SPP1 NRS5065 → NRS2097 |
| NRS4552 | 168 *amyE*::P$_{hy\text{-}spank}$-*bslA*$_{L119K}$-*lacI (spc)* | pNW1190 →168 |
| NRS4553 | 168 *amyE*::P$_{hy\text{-}spank}$-*bslA*$_{L121K}$-*lacI (spc)* | pNW1191 →168 |
| NRS4554 | 168 *amyE*::P$_{hy\text{-}spank}$-*bslA*$_{L123K}$-*lacI (spc)* | pNW1192 →168 |
| NRS4555 | 168 *amyE*::P$_{hy\text{-}spank}$-*bslA*$_{L124K}$-*lacI (spc)* | pNW1193 →168 |
| NRS4556 | 168 *amyE*::P$_{hy\text{-}spank}$-*bslA*$_{L153K}$-*lacI (spc)* | pNW1194 →168 |
| NRS4557 | 168 *amyE*::P$_{hy\text{-}spank}$-*bslA*$_{I155K}$-*lacI (spc)* | pNW1195 →168 |
| NRS4559 | 3610 *bslA*::*cat amyE*::P$_{hy\text{-}spank}$-*bslA*$_{L119K}$-*lacI (spc)* | SPP1 NRS4552 → NRS2097 |
| NRS4561 | 3610 *bslA*::*cat amyE*::P$_{hy\text{-}spank}$-*bslA*$_{L121k}$-*lacI (spc)* | SPP1 NRS4553 → NRS2097 |
| NRS4563 | 3610 *bslA*::*cat amyE*::P$_{hy\text{-}spank}$-*bslA*$_{L123K}$-*lacI (spc)* | SPP1 NRS4554 → NRS2097 |
| NRS4565 | 3610 *bslA*::*cat amyE*::P$_{hy\text{-}spank}$-*bslA*$_{L124K}$-*lacI (spc)* | SPP1 NRS4555 → NRS2097 |
| NRS4567 | 3610 *bslA*::*cat amyE*::P$_{hy\text{-}spank}$–*bslA*$_{L153K}$-*lacI (spc)* | SPP1 NRS4556 → NRS2097 |
| NRS4569 | 3610 *bslA*::*cat amyE*::P$_{hy\text{-}spank}$-*bslA*$_{I155K}$-*lacI (spc)* | SPP1 NRS4557 → NRS2097 |
| Plasmid | | |
| pUC19 | High-copy-number cloning vector | 7 |
| pDR111 | *B. subtilis* integration vector for IPTG-induced expression | 8 |
| pGEX-6P-1 | Vector for overexpression of GST-fused proteins | GE Healthcare |
| pNW518 | pDR111-*bslA* | 4 |
| pNW690 | pUC19-*bslA* | This work |
| pNW693 | pUC19-*bslA*$_{L76I}$ | This work |
| pNW1104 | pDR111-*bslA*$_{L76I}$ | This work |
| pNW1128 | pGEX-6P-1-TEV-*bslA*$_{42–181}$ | This work |
| pNW1129 | pUC19-*bslA*$_{L76D}$ | This work |
| pNW1136 | pUC19-*bslA*$_{L76K}$ | This work |
| pNW1143 | pDR111-*bslA*$_{L76D}$ | This work |
| pNW1144 | pDR111-*bslA*$_{L76K}$ | This work |
| pNW1149 | pUC19-*bslA*$_{L79K}$ | This work |
| pNW1150 | pUC19-*bslA*$_{L79D}$ | This work |
| pNW1151 | pUC19-*bslA*$_{L79I}$ | This work |

**Table S3. Cont.**

| Strain, plasmid, or primer | Relevant genotype/description | Source/construction*,† |
|---|---|---|
| pNW1157 | pDR111-*bslA*$_{L79D}$ | This work |
| pNW1158 | pDR111-*bslA*$_{L79I}$ | This work |
| pNW1160 | pGEX-6P-1-*bslA*$_{48–172,\ L98M}$ | This work |
| pNW1162 | pGEX-6P-1-TEV-*bslA*$_{42–181,\ L79K}$ | This work |
| pNW1165 | pDR111-*bslA*$_{L79K}$ | This work |
| pNW1174 | pUC19-*bslA*$_{L98M}$ | This work |
| pNW1175 | pUC19-*bslA*$_{L77I}$ | This work |
| pNW1176 | pUC19-*bslA*$_{L77K}$ | This work |
| pNW1177 | pUC19-*bslA*$_{L77D}$ | This work |
| pNW1178 | pDR111-*bslA*$_{L98M}$ | This work |
| pNW1179 | pDR111-*bslA*$_{L77I}$ | This work |
| pNW1180 | pDR111-*bslA*$_{L77K}$ | This work |
| pNW1461 | pDR111-*bslA*$_{L77D}$ | This work |
| pNW1182 | pUC19-*bslA*$_{L119K}$ | This work |
| pNW1183 | pUC19-*bslA*$_{L121K}$ | This work |
| pNW1184 | pUC19-*bslA*$_{L123K}$ | This work |
| pNW1185 | pUC19-*bslA*$_{L124K}$ | This work |
| pNW1186 | pUC19-*bslA*$_{L153K}$ | This work |
| pNW1187 | pUC19-*bslA*$_{I155K}$ | This work |
| pNW1188 | pGEX-6-P-TEV-*bslA*$_{42–181,\ L76K}$ | This work |
| pNW1189 | pGEX-6-P-TEV-*bslA*$_{42–181,\ L77K}$ | This work |
| pNW1190 | pDR111-*bslA*$_{L119K}$ | This work |
| pNW1191 | pDR111-*bslA*$_{L121K}$ | This work |
| pNW1192 | pDR111-*bslA*$_{L123K}$ | This work |
| pNW1193 | pDR111-*bslA*$_{L124K}$ | This work |
| pNW1194 | pDR111-*bslA*$_{L153K}$ | This work |
| pNW1195 | pDR111-*bslA*$_{I155K}$ | This work |
| pNW1196 | pGEX-6P-1-*bslA*$_{48–172}$ | This work |
| Primer | Sequence 5′ – 3′ | Use |
| NSW1337 | TACCGTCCAAACACGATTCTCAGCCTTGGCG | L76I mutagenesis |
| NSW1338 | CGCCAAGGCTGAGAATCGTGTTTGGACGGTA | L76I mutagenesis |
| NSW1517 | GCATCTCGAGTTATTAGTTGCAACCGCAAGGC | *bslA*$_{42–181}$ cloning |
| NSW1537 | CAGGGGCCCCTGGGATCCGAAAATTTATATTTTCAAATGAGAACACAGTCTACA | *bslA*$_{42–181}$ cloning |
| NSW1539 | TTACCGTCCAAACACGAAACTCAGCCTTGGCGTTA | L76K mutagenesis |
| NSW1540 | TAACGCCAAGGCTGAGTTTCGTGTTTGGACGGTAA | L76K mutagenesis |
| NSW1541 | TTACCGTCCAAACACGGATCTCAGCCTTGGCGTTA | L76D mutagenesis |
| NSW1542 | TAACGCCAAGGCTGAGATCCGTGTTTGGACGGTAA | L76D mutagenesis |
| NSW1571 | AAACACGCTTCTCAGCATTGGCGTTATGGAGTTTA | L79I mutagenesis |
| NSW1572 | TAAACTCCATAACGCCAATGCTGAGAAGCGTGTTT | L79I mutagenesis |
| NSW1573 | AAACACGCTTCTCAGCAAAGGCGTTATGGAGTTTA | L79K mutagenesis |
| NSW1574 | TAAACTCCATAACGCCTTTGCTGAGAAGCGTGTTT | L79K mutagenesis |
| NSW1575 | AAACACGCTTCTCAGCGATGGCGTTATGGAGTTTA | L79D mutagenesis |
| NSW1576 | TAAACTCCATAACGCCATCGCTGAGAAGCGTGTTT | L79D mutagenesis |
| NSW1585 | AAACACGAAAGACACAATGAACGGAAATGCCTTGC | L98M mutagenesis |
| NSW1586 | GCAAGGCATTTCCGTTCATTGTGTCTTTCGTGTTT | L98M mutagenesis |
| NSW1591 | CCGTCCAAACACGCTTATTAGCCTTGGCGTTATGG | L77I mutagenesis |
| NSW1592 | CCATAACGCCAAGGCTAATAAGCGTGTTTGGACGG | L77I mutagenesis |
| NSW1593 | CCGTCCAAACACGCTTAAAAGCCTTGGCGTTATGG | L77K mutagenesis |
| NSW1594 | CCATAACGCCAAGGCTTTTAAGCGTGTTTGGACGG | L77K mutagenesis |
| NSW1595 | CCGTCCAAACACGCTTGATAGCCTTGGCGTTATGG | L77D mutagenesis |
| NSW1596 | CCATAACGCCAAGGCTATCAAGCGTGTTTGGACGG | L77D mutagenesis |
| NSW1597 | AACAGTAAGAGTTCCTAAAGCACTTGATTTGTTAG | L119K mutagenesis |
| NSW1598 | CTAACAAATCAAGTGCTTTAGGAACTCTTACTGTT | L119K mutagenesis |
| NSW1599 | AAGAGTTCCTTTGGCAAAAGATTTGTTAGGAGCTG | L121K mutagenesis |
| NSW1704 | CAGCTCCTAACAAATCTTTTGCCAAAGGAACTCTT | L121K mutagenesis |
| NSW1705 | TCCTTTGGCACTTGATAAATTAGGAGCTGGCGAAT | L123K mutagenesis |
| NSW1706 | ATTCGCCAGCTCCTAATTTATCAAGTGCCAAAGGA | L123K mutagenesis |
| NSW1707 | TTTGGCACTTGATTTGAAAGGAGCTGGCGAATTCA | L124K mutagenesis |
| NSW1708 | TGAATTCGCCAGCTCCTTTCAAATCAAGTGCCAAA | L124K mutagenesis |
| NSW1709 | TGCGGAGAATAAATCAAAAAGCATCGGAAATAAAT | L153K mutagenesis |
| NSW1710 | ATTTATTTCCGATGCTTTTTGATTTATTCTCCGCA | L153K mutagenesis |
| NSW1711 | GAATAAATCATTAAGCAAAGGAAATAAATTTTACG | I155K mutagenesis |

**Table S3. Cont.**

| Strain, plasmid, or primer | Relevant genotype/description | Source/construction*,† |
|---|---|---|
| NSW1712 | CGTAAAATTTATTTCCTTTGCTTAATGATTTATTC | I155K mutagenesis |
| NSW1713 | CTGTTCCAGGGGCCCCTGGGATCCGCTTCATTGTTCGCAACAATCAC | $bslA_{48–172}$ cloning |
| NSW1714 | CTCGAGTTAGTTGCAACCGCATCATTAAGTGCTGCGCTTAGCCACGTC | $bslA_{48–172}$ cloning |

*BSGC represents the *Bacillus* genetic stock center.
†The direction of strain construction is indicated with DNA or phage (SPP1) (→) recipient strain.


1. Studier FW, Moffatt BA (1986) Use of bacteriophage T7 RNA polymerase to direct selective high-level expression of cloned genes. *J Mol Biol* 189(1):113–130.
2. Perego M, Spiegelman GB, Hoch JA (1988) Structure of the gene for the transition state regulator, *abrB*: Regulator synthesis is controlled by the *spo0A* sporulation gene in *Bacillus subtilis*. *Mol Microbiol* 2(6):689–699.
3. Verhamme DT, Kiley TB, Stanley-Wall NR (2007) DegU co-ordinates multicellular behaviour exhibited by *Bacillus subtilis*. *Mol Microbiol* 65(2):554–568.
4. Verhamme DT, Murray EJ, Stanley-Wall NR (2009) DegU and Spo0A jointly control transcription of two loci required for complex colony development by *Bacillus subtilis*. *J Bacteriol* 191 (1):100–108.
5. Ostrowski A, Mehert A, Prescott A, Kiley TB, Stanley-Wall NR (2011) YuaB functions synergistically with the exopolysaccharide and TasA amyloid fibers to allow biofilm formation by *Bacillus subtilis*. *J Bacteriol* 193(18):4821–4831.
6. Murray EJ, Strauch MA, Stanley-Wall NR (2009) SigmaX is involved in controlling Bacillus subtilis biofilm architecture through the AbrB homologue Abh. *J Bacteriol* 191(22):6822–6832.
7. Yanisch-Perron C, Vieira J, Messing J (1985) Improved M13 phage cloning vectors and host strains: Nucleotide sequences of the M13mp18 and pUC19 vectors. *Gene* 33(1):103–119.
8. Britton RA, et al. (2002) Genome-wide analysis of the stationary-phase sigma factor (sigma-H) regulon of *Bacillus subtilis*. *J Bacteriol* 184(17):4881–4890.


**Movie S1.** Pendant drop analysis of in vitro self-assembly of wild-type recombinant $BslA_{42-181}$ protein. A 40-μL drop of BslA is expelled into an oil bath, 5 μL is retracted and the elastic skin is seen at the protein-oil interface, as evidenced by the wrinkle formation around the neck of the drop. No relaxation of the wrinkles is observed, showing the stability of the surface layer.

Movie S1

**Movie S2.** Pendant drop analysis of in vitro self-assembly of recombinant $BslA_{42-181}$ protein containing the L76K mutation. A 40-μL drop of BslA is expelled into an oil bath, 5 μL is retracted and the elastic skin is seen at the protein-oil interface, as evidenced by the wrinkle formation around the neck of the drop. Gradual relaxation of the wrinkles can be seen, indicating a slight loss of surface layer stability compared with wild-type protein.

Movie S2

**Movie S3.** Pendant drop analysis of in vitro self-assembly of recombinant $BslA_{42\text{-}181}$ protein containing the L77K mutation. A 40-μL drop of BslA is expelled into an oil bath, 5 μL is retracted and the elastic skin is seen at the protein-oil interface, as evidenced by the wrinkle formation around the neck of the drop. Relaxation of the wrinkles can be seen, indicating a loss of surface layer stability compared with wild-type protein.

Movie S3

**Movie S4.** Pendant drop analysis of in vitro self-assembly of recombinant $BslA_{42\text{-}181}$ protein containing the L79K mutation. A 40-μL drop of BslA is expelled into an oil bath, 5 μL is retracted and the elastic skin is seen at the protein-oil interface, as evidenced by the wrinkle formation around the neck of the drop. Gradual relaxation of the wrinkles can be seen, indicating a slight loss of surface layer stability compared with wild-type protein.

Movie S4